Since January 2020 Elsevier has created a COVID-19 resource centre with free information in English and Mandarin on the novel coronavirus COVID-19. The COVID-19 resource centre is hosted on Elsevier Connect, the company's public news and information website.

Genomics 113 (2021) 2177–2188

Contents lists available at ScienceDirect

Genomics

journal homepage: www.elsevier.com/locate/ygeno

Original Article

Comparative analysis of human coronaviruses focusing on nucleotide variability and synonymous codon usage patterns

Jayanta Kumar Das [a,*], Swarup Roy [b,*]

[a] Department of Pediatrics, Johns Hopkins University School of Medicine, MD, USA
[b] Network Reconstruction & Analysis (NetRA) Lab, Department of Computer Applications, Sikkim University, Gangtok, India

ARTICLE INFO

Keywords:
Nucleotide
Codon
RSCU
Amino acid
Phylogeny
Coronaviruses

ABSTRACT

The prevailing COVID-19 pandemic has drawn the attention of the scientific community to study the evolutionary origin of Severe Acute Respiratory Syndrome Corona Virus 2 (SARS-CoV-2). This study is a comprehensive quantitative analysis of the protein-coding sequences of seven human coronaviruses (HCoVs) to decipher the nucleotide sequence variability and codon usage patterns. It is essential to understand the survival ability of the viruses, their adaptation to hosts, and their evolution.

The current analysis revealed a high abundance of the relative dinucleotide (odds ratio), GC and CT pairs in the first and last two codon positions, respectively, as well as a low abundance of the CG pair in the last two positions of the codon, which might be related to the evolution of the viruses. A remarkable level of variability of GC content in the third position of the codon among the seven coronaviruses was observed. Codons with high RSCU values are primarily from the aliphatic and hydroxyl amino acid groups, and codons with low RSCU values belong to the aliphatic, cyclic, positively charged, and sulfur-containing amino acid groups. In order to elucidate the evolutionary processes of the seven coronaviruses, a phylogenetic tree (dendrogram) was constructed based on the RSCU scores of the codons. The severe and mild categories CoVs were positioned in different clades. A comparative phylogenetic study with other coronaviruses depicted that SARS-CoV-2 is close to the CoV isolated from pangolins (*Manis javanica*, Pangolin-CoV) and cats (*Felis catus*, SARS(r)-CoV). Further analysis of the effective number of codon (ENC) usage bias showed a relatively higher bias for SARS-CoV and MERS-CoV compared to SARS-CoV-2. The ENC plot against GC3 suggested that the mutational bias might have a role in determining the codon usage variation among candidate viruses.

A codon adaptability study on a few human host parasites (from different kingdoms), including CoVs, showed a diverse adaptability pattern. SARS-CoV-2 and SARS-CoV exhibit relatively lower but similar codon adaptability compared to MERS-CoV.

1. Introduction

Coronavirus (CoV) is a large, enveloped virus (family-*Coronaviridae*, subfamily-*Coronavirinae*) with non- segmented, single-stranded and positive-sense RNA genomes [1]. Seven coronaviruses have been known to infect a human host and cause respiratory diseases. The severe acute respiratory syndrome coronavirus (SARS-CoV) and Middle-East respiratory syndrome coronavirus (MERS-CoV) are the two most lethal coronaviruses. SARS-CoV was first reported in China in 2002 [2,3] and caused about 2000 deaths worldwide. MERS-CoV was reported in Saudi Arabia and South Korea in 2012 and 2015, respectively [4,5]. SARS-CoV-2 is the most recently reported novel CoV (2019), which provoked a large-scale COVID-19 epidemic. SARS-CoV-2 was originated from Wuhan, the largest metropolitan area in the Hubei province in China. SARS-CoV-2 is highly infectious due to its high dissemination rate worldwide. According to the World Health Organization (WHO) report,[1] more than 600,000 people were deceased as of July 15, 2020, due to COVID-19. All the three coronaviruses are highly pathogenic, resulting in global outbreaks. The other four human coronaviruses (HCoVs), such as OC43 (HCoV- OC43), HKU1 (HCoV-HKU1), 229E (HCoV-229E), and NL63 (HCoV-NL63), are considered to be a mild category due to their low infection and mortality rate.

* Corresponding authors.
E-mail addresses: dasjayantakumar89@gmail.com (J.K. Das), sroy01@cus.ac.in (S. Roy).
[1] https://www.worldometers.info/coronavirus/

https://doi.org/10.1016/j.ygeno.2021.05.008
Received 19 July 2020; Received in revised form 9 May 2021; Accepted 14 May 2021
Available online 19 May 2021

The complete genome length of SARS-CoV, SARS-CoV-2, and MERS-CoV is approximately 27–30 kbp. The genome of SARS-CoV-2 shows a high sequence similarity (79%) with SARS-CoV and relatively low similarity (50%) with MERS-CoV [6]. The several putative coding regions available in SARS-CoV-2, encode essential genes that include nonstructural proteins such as orf1ab, structural proteins namely spike glycoprotein (S), envelope (E), membrane (M), and nucleocapsid (N), and several accessory protein chains [2,7–9]. The two-third of the genome is at the 5′-end of the sequence, encoding the nonstructural proteins, and one-third is at the 3′-end, encoding four structural proteins [7]. The CoV proteins exert diverse functional roles, while nonstructural proteins block the host's innate immune response [10], the four structural proteins show various functionalities. For example, the envelope protein promotes viral assembly and release [11], spike protein composes the spikes on the viral surface and helps in binding with host receptors [11], nucleocapsid protein self-associates through a C-terminal and activates the expression of cyclooxygenase-2 [12,13], and membrane protein promotes the membrane fusion, regulates viral replication, and packs genomic RNA into viral particles [14,15]. On the other hand, accessory proteins that play a significant role during CoV infection contain several overlapping regions that have been explored slightly; these usually play significant roles during coronavirus infection [16]. However, the accessory proteins may not be functional [17]. Several sequence variability features of structural and nonstructural proteins are yet to be investigated thoroughly.

A total of 61 codons genetically code 20 standard amino acids, and the remaining three codons are for the translation of the termination signal [18]. Therefore, a single amino acid can be coded by multiple codons, which are termed as *synonymous codons*. The number of synonymous codons for different amino acids varies between 1 and 6. The virus genome differs from each other due to frequent mutations that can prevent the PCR from binding to target sequences [19]. Similar to other RNA viruses, SARS-CoV-2 mutates [20] and creates diverse functionality [21]. Mutation plays a key role that triggers a zoonotic virus to jump from animal to human host [22]. Due to several other biological factors, the mechanism of pathogenicity might differ in highly pathogenic strains that diversify the virus target hosts, even in closely related strains [23,24]. Genome-wide codon usage signature can predict evolutionary forces [25]. The inter- and intra-species codon usage patterns may vary significantly in different organisms [26]. Therefore, it is genetically important to study the nucleotide base composition in all three positions of codon as it could influence the codon usage and mutational bias [27–29]. The frequency of the dinucleotide features is also critical as it might affect the usage of codons [27,30]. Thus, GC (G + C) content may be a good indicator towards understanding the expression of viral genes while interacting with the host proteins [31,32].

Previous studies have demonstrated that the usage of a synonymous codon is a non-random procedure [33,34]. The relative synonymous codon usage (RSCU) standardizes the codon usage of the amino acids encoded by multiple codons. The RSCU value is independent of the amino acid composition and has been used widely to estimate the codon usage bias. Several studies have been performed on CoVs, primarily focusing on the independent genome [27,35] and different strains within the same genome [36]. The recent studies on SARS-CoV-2 have focused on elucidating the proximal origin of SARS-CoV-2 and the host-specific adaption mechanism [37–39]. A study on the codon usage pattern provided an insight into the evolution of viruses and their adaption to hosts [40]. However, several crucial roles are yet to be unveiled from all CoVs, including SARS-CoV-2, to fight against COVID-19 related diseases. Therefore, a genomic level comparative study could help in understanding the molecular and structural resemblance among all HCoVs.

The present study emphasized a comprehensive and integrated study on seven HCoVs. Several bias indexing measures, such as nucleotide composition, dinucleotide odds ratio [41], relative synonymous codon usage pattern [42], effective number of codon usage [43,44], and codon adaptation [45,46] are used to quantify the variability of the candidate HCoVs.

Table 1
Seven strains of HCoVs with collected number of unique sequences and total protein coding genes in each strains.

Human coronaviruses	Number of unique sequences	Number of protein coding genes
SARS-CoV	134	1766
SARS-CoV-2	401	4525
MERS-CoV	233	2509
HCoV-OC43	157	1257
HCoV-HKU1	34	277
HCoV-229E	29	225
HCoV-NL63	56	389

2. Material and methods

2.1. Data retrieval and filtering

The seven candidate species of HCoVs, used in this study, are known to infect the human host. For this research, the nucleotide sequences each of length ≈28*kb* are collected for candidate viruses from NCBI database[2] during April 2020 (Supplementary material 1). All the partial, incomplete, and duplicate genome sequences were removed. Then, for each complete sequence, the single coding sequences are obtained by concatenating the coding regions of all the genes, *Orf1ab, S, E, M, N, Orf3a, Orf3b, Orf6, Orf7a, Orf7b, Orf8(a/b)*, and *Orf10* (length 150 bp). The sequence general information for our study are summarized in Table 1.

2.2. Quantitative measuring indices of nucleotide composition

We reported some of the popular quantitative measuring indices to quantify the composition variability (or similarity) among seven CoVs.

2.2.1. Quantifying nucleotide composition

The quantity of nucleotide base composition (A, T, C, and G) in three different codon positions can be calculated based on the frequency. The base composition and GC-content at the first (GC1), second (GC2), and third positions (GC3) of synonymously variable sense codons vary from 0 to 1. The nucleotide composition of any nucleotide X at position P can be calculated as follows:

$$N_X(P) = \frac{f_x}{f_A + f_T + f_C + f_G}, \tag{1}$$

where, $X \in \{A, T, C, G\}$, $p \in 1,2,3$ and f_A, f_T, f_C, f_G are the nucleotide frequencies at particular position P for A, T, C and G respectively.

Similarly, we calculated the pair nucleotide composition in a particular position P as follows:

$$N_{XY}(P) = \frac{f_x + f_y}{f_A + f_T + f_C + f_G}, \tag{2}$$

where, $X, Y \in \{A, T, C, G\}$.

2.2.2. Relative dinucleotide abundance

Dinucleotide (DN) composition and variability are essential as they represent the possible bonding and abundance of two consecutive nucleotides over the sequences. In RNA viruses, the relative abundance of dinucleotide has been shown to affect codon usage [28]. The dinucleotide frequency is often used to determine the favorable or unfavorable nucleotide pairs. The patterns of dinucleotide frequency indicate both

[2] https://www.ncbi.nlm.nih.gov/

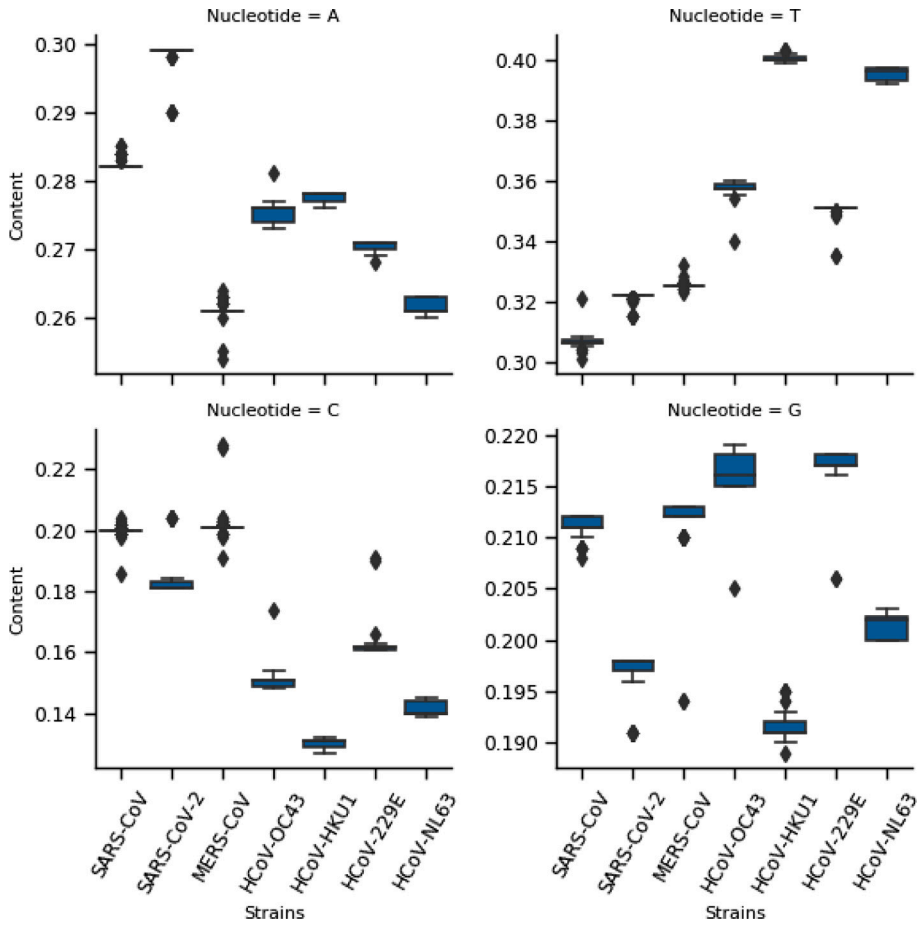

Fig. 1. Box plot showing the distribution of four nucleotide content (A/T/C/G) for seven HCoVs.

selection and mutational pressures [27,47]. The total possible dinucleotide combinations are 16. The relative dinucleotide abundance frequency can be calculated as follows:

$$D_{xy} = \frac{f_{xy}}{f_x f_y}, \tag{3}$$

where, f_x and f_y represent the individual frequency of nucleotides x and y respectively, and f_{xy} is the frequency of dinucleotide xy in the same sequence. The ratio of observed to expected dinucleotide frequency is known as the *odds ratio*. The odds ratio $\leq$0.78 indicated that dinucleotide is underrepresented, whereas a value of $\geq$1.25 indicates overrepresentation [41].

2.2.3. Relative synonymous codon usage (RSCU)-pattern

RSCU is the ratio between the observed number of codons and the expected uniform synonymous codon usage [42] (Eq. (4)). The RSCU is used to standardize the codon usage of these amino acids encoded by multiple codons. The RSCU value is independent of the amino acid composition and has been used widely to estimate the codon usage bias. The RSCU value $\geq$1.0 is considered a positive codon usage bias, and the value $\leq$1.0 is considered a negative codon usage bias. Thus, a high RSCU value for a codon indicates frequent usage of that codon.

$$RSCU_{i,j} = \frac{X_{i,j}}{\frac{1}{n}\sum_{j=1}^{n_i} X_{i,j}}, \tag{4}$$

where, X_i is the number of occurrences of the j^{th} codon for the i^{th} amino acid, which is encoded by n_i synonymous codons.

2.2.4. Effective number of codon (ENC) usage

The *ENC* (or N_c) usage can be obtained by Eq. (5) [43,44].

$$N_c = 2 + \frac{9}{\widehat{F}_2} + \frac{1}{\widehat{F}_3} + \frac{5}{\widehat{F}_4} + \frac{3}{\widehat{F}_6}, \tag{5}$$

where F_i denotes the average homozygosity for the class with i synonymous codons. The *ENC* value ranges from 20 to 61. An *ENC* of 20 represents extreme bias as only one codon is used for each amino acid, and a value of 61 suggests no bias. In contrast to the RSCU value, a high *ENC* value correlates to a weak codon usage bias. An alternate approach for calculating the *ENC* is based on the GC3-content, shown in Eq. (6).

$$N_c = 2 + s + \left\{29 \Big/ \left[s^2 + (1-s)^2\right]\right\} \tag{6}$$

2.2.5. Neutrality plot

A neutrality plot is an analytical method for assessing codon usage to account for mutation-selection equilibrium. A dot in the plot represents each independent sequence. In this plot, the mean GC-content at the third codon position (X-axis), represented by GC3, is compared to the mean GC-content at the first and second codon positions, represented by GC12 (Y-axis). The slope of a regression line represents the effect of mutation pressure on the biased usage of codons. A regression line close to 1 implies mutation bias as a central force for influencing the codon usage [48].

Typically, the correlation, r (or R) indicates the strength of the linear association between two variables (x and y). In current study, we considered x and y as the GC-content in different codon positions (GC3, GC12, GC1, and GC2). The R^2 value indicated the amount of variability in y, explained by the predictor (regressor) x. The R^2 value always ranges between 0 and 1.

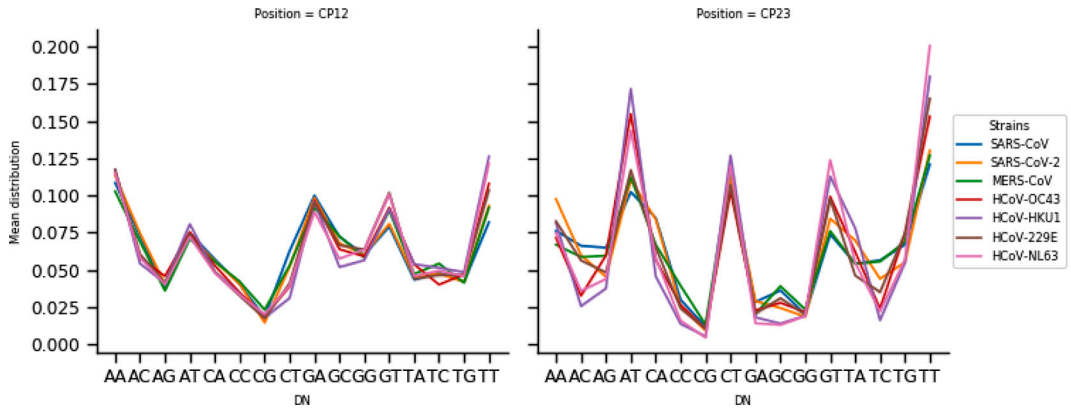

Fig. 2. Distribution of mean (average) dinucleotide (DN) content. The mean DN is calculated for both the first two codon positions (CP12) and the last two codon positions (CP23) for seven HCoVs.

2.2.6. Codon adaptation index (CAI)

The CAI is a measure of the synonymous codon usage bias for a DNA or RNA sequence. It quantifies the similarity between the synonymous codon usage of a gene and the synonymous codon frequency of a reference set [45,46]. The CAI value ranges from 0 to 1; 1 indicates if a gene always uses the most frequently used synonymous codons in the reference set. Therefore, it can be used to understand the codon adaptability between the host and parasite [49,50].

3. Results and discussion

This section highlights the comparative distribution of nucleotide and dinucleotide features in all the HCoVs. Then, codon usage bias (RSCU) was estimated among candidate gene sequences. The RSCU features are used for establishing a phylogenetic relation among the candidate species. Finally, the correlation score was calculated between GC3 and GC content at various codon positions.

3.1. Variability of nucleotide composition

The variability of nucleotide composition is shown using a box-plot in Fig. 1. Notably, the virus nucleotide composition differs significantly with highly diverse base composition of the MERS-CoV genome. Next, we focused on the high and low abundance of four nucleotide bases in seven candidate strains. In addition, a high abundance of base A in SARS-CoV-2 and low in MERS-CoV and HCoV-NL63 was observed. Base T was highly available in HCoV-HKU1 and HCoV-NL63, whereas low in SARS-CoV. SARS-CoV and MERS-CoV contained a high content of base C, while a low availability of base C was detected in HCoV-HKU1. Similarly, the G content was high in HCoV-OC43 and HCoV-229E and low in HCoV-HKU1. General trends of CDSs of all CoV strains were found to be rich in A and T (58 – 67%) compared to G and C nucleotides. This characteristic was similar to that of the *Nipah* virus [27], although, we observed a higher abundance of T than A in their genome.

3.2. Dinucleotide (DN) variability and usage pattern

We focused on both the first two codon positions (CP12) and the last two codon positions (CP23) to quantitate the consecutive nucleotide pairs (dinucleotide). The observed frequency distribution of nucleotide pair is shown in Fig. 2. We observed a high abundance of nucleotide pairs (AA, GA, GT, and TT) in CP12, when compared to high abundance nucleotide pairs (AT, CT, GT, and TT) in CP23. It is worth mentioning here that dinucleotides, GA and CT, belong to *purine* and *pyrimidine* groups, respectively. We also observed less variability in the nucleotide pairs in the CP23 position than CP12 (Fig. 2) position across the seven viruses. Overall, this indicates a distinct pattern of nucleotide pairs in two consecutive codon positions.

Table 2
Top two high and low usage dinucleotide (DN) odds ratio scores for both the combination of codon positions (first two codon positions-CP12 and the last two codon positions-CP23).

	Odds ratio (codon position: CP12)							
	High usage				Low usage			
Virus	DN	Value	DN	Value	DN	Value	DN	Value
SARS-CoV	GC	1.50	GA	1.41	AG	0.53	CG	0.38
SARS-CoV-2	GC	1.48	GA	1.39	TA	0.56	CG	0.31
MERS-CoV	GC	1.49	GT	1.41	AG	0.53	CG	0.47
HCoV-OC43	GC	1.55	TT	1.36	AG	0.62	CG	0.47
HCoV-HKU1	GC	1.40	GA	1.37	TA	0.58	CG	0.48
HCoV-229E	GC	1.55	GT	1.46	AG	0.56	CG	0.40
HCoV-NL63	GC	1.41	GT	1.41	TA	0.53	CG	0.49
	Odds ratio (codon position: CP23)							
SARS-CoV	CA	1.46	AG	1.45	TA	0.56	CG	0.34
SARS-CoV-2	GT	1.60	CT	1.59	TC	0.62	CG	0.33
MERS-CoV	CT	1.49	AG	1.45	GA	0.49	CG	0.37
HCoV-OC43	CT	1.63	GT	1.43	CG	0.40	TC	0.38
HCoV-HKU1	CT	2.12	GT	1.75	CG	0.29	TC	0.27
HCoV-229E	CT	1.51	GT	1.51	GA	0.49	CG	0.36
HCoV-NL63	CT	1.83	GT	1.83	TC	0.34	CG	0.21

Furthermore, we reported the relative abundance of dinucleotide content (odds ratio) for the two highest and lowest usage nucleotide pairs in Table 2. Quantitatively, we observed a similar pattern for the highest and lowest usage nucleotide pairs (GC and CG, respectively) in CP12 position across the seven strains. A similar observation was reported for MERS-CoV [36]. However, we found different structures for the second-highest and lowest usage of nucleotide pairs. We also observed a distinct arrangement of high usage (CT) and low usage (CG) nucleotide pairs in CP23 in the majority of viruses and is also different from the CP12 position as stated above. These two high-usage dinucleotides, GC (in CP12) and CT (in CP23), belong to *strong* and *pyrimidine* groups.

3.3. GC content usage pattern

GC content at three different codon positions was calculated for each sequence. We obtained mean (or average) GC content and standard deviation for each strain of CoVs as shown in Table 3. It was calculated using Eq. (2). Interestingly, we observed that GC3 shows a high variability among seven viruses, although the GC content in GC1 and GC2 was much greater than that of GC3. Pairwise, the mean GC content for SARS-CoV, MERS-CoV, SARS-CoV-2, and HCoV-229E appeared to be identical. The position-wise GC-content distribution was examined

Table 3
GC content variability in seven HCoVs is shown by highlighting mean and standard deviation for each codon positions (first codon position-GC1, second codon position-GC2, third codon position-GC3).

	GC1		GC2		GC3		GC	
Virus	mean	std	mean	std	mean	std	mean	std
SARS-CoV	0.4902	0.0018	0.3918	0.0009	0.3520	0.0034	0.4113	0.0017
SARS-CoV-2	0.4700	0.0001	0.3876	0.0025	0.2818	0.0038	0.3796	0.0021
MERS-CoV	0.4860	0.0011	0.3973	0.0027	0.3575	0.0021	0.4135	0.0013
HCoV-229E	0.4667	0.0014	0.3750	0.0059	0.2987	0.0088	0.3802	0.0046
HCoV-HKU1	0.4262	0.0035	0.3546	0.0025	0.1854	0.0020	0.3220	0.0009
HCoV-NL63	0.4514	0.0012	0.3678	0.0016	0.2105	0.0034	0.3433	0.0013
HCoV-OC43	0.4569	0.0020	0.3676	0.0026	0.2769	0.0026	0.3669	0.0014

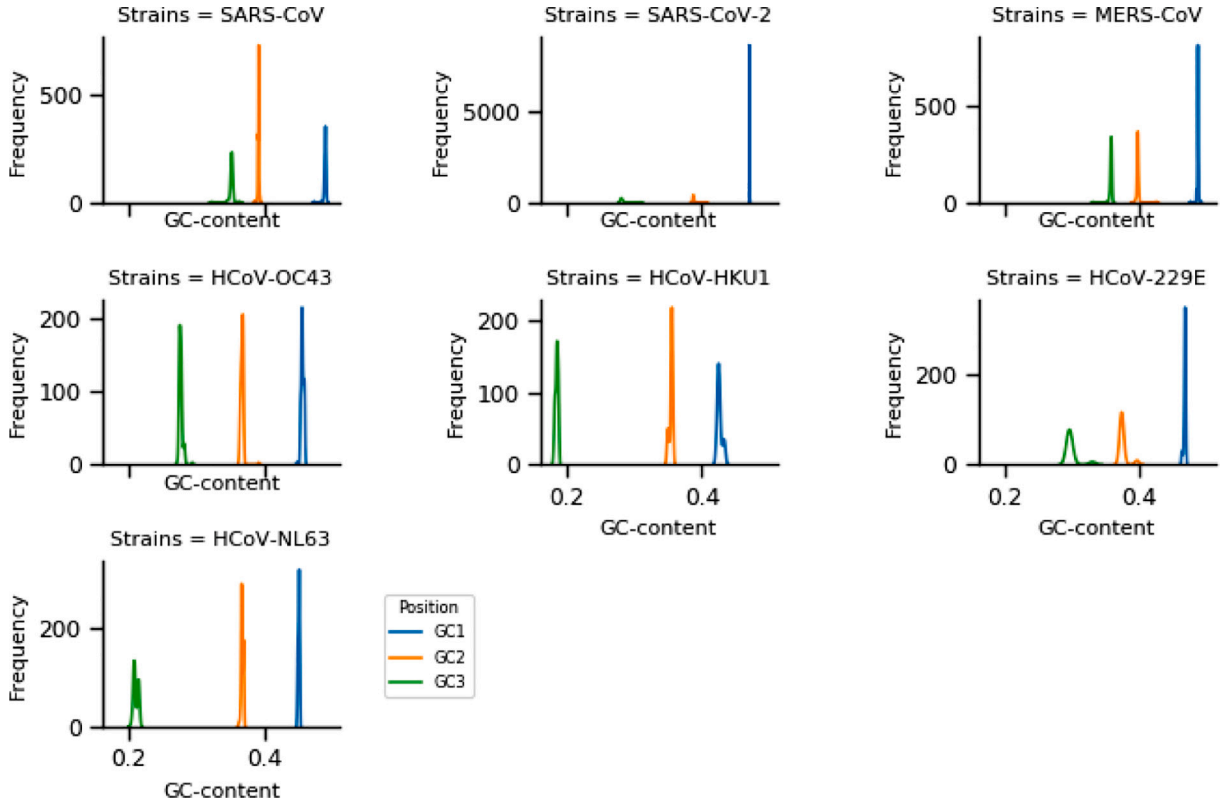

Fig. 3. The distribution of GC-content in three codon positions (first codon position-GC1, second codon position-GC2, third codon position-GC3) for all seven HCoVs.

(Fig. 3). We observed that GC content in the three codon positions is well-balanced for HCoV-OC43 and SARS- CoV-2 (mean difference ≈0.9), whereas HCoV-HKU1 and HCoV-NL63 showed similar GC-content between the first and second positions of the codon (mean difference <0.9), and SARS-CoV, MERS-CoV, and HCoV-229E showed a similar GC content trend in the second and third positions of the codon (mean difference <0.9).

3.4. Synonymous codon usage pattern and phylogenetic clustering

We calculated the RSCU values of 59-non trivial codons (Eq. (4)). The RSCU value for each amino acid and synonymous codons are shown in Table 4, and the distribution pattern is shown in Fig. 4. Next, a high RSCU score (>1.5) and a low RSCU score (<0.5) were obtained for all the seven CoVs. Overall, the comparison of SARS-CoV-2's RSCU values to those of the SARS-CoV and MERS-CoV revealed a similar pattern for most of the codons [36,51].

High RSCU score codons: The number of codons with high RSCU value in the seven viruses were as follows: SARS-CoV (13), SARS-CoV-2 (14), MERS-CoV (9), HCoV-OC43 (18), HCoV-HKU1 (18), HCoV-229E (11), and HCoV-NL63 (18). Interestingly, a maximum of 18 codons was detected in the mild category of CoVs (HCoV-OC43, HCoV-HKU1, and HCoV-NL63) with high RSCU values, while a minimum of 9 codons was detected in one severe category, MERS-CoV with high RSCU values. In the severe category coronaviruses, high RSCU value codons were mapped to 10 amino acids (A, C, G, I, L, P, R, S, T, and V). However, in the case of mild category CoVs, codons were mapped to the same set of amino acids as in severe category, with an additional five amino acids (D, F, H N, and Y). Together, we observed only 7 common codons among the seven HCoVs: ATT, ACT, TCT, CCT, GTT, GCT, and GGT. Among these 7 codons, 4 were from the aliphatic amino acid group (I-ATT, V-GTT, A-GCT, G-GGT), 2 were from the sulfur-containing amino acid group (S-TCT and T-ACT), and 1 is from the cyclic amino acid group (P-CCT) (Table 4) according to the 8 chemical groups of amino acid categorization [52,53]. On the other hand, significant differences were obtain in the frequencies of two glutamine codons (GAG and GAA) among SARS-CoV-2 and SARS and MERS-CoVs (Table 4).

Low RSCU score codons: The number of codons with low RSCU values in 7 viruses were as follows: SARS-CoV (9), SARS- CoV-2 (13), MERS-CoV (10), HCoV-OC43 (19), HcoV-HKU1 (27), HcoV-229E (19),

Table 4
RSCU score for various amino acids (AA) and corresponding synonymous codons for seven HCoVs. The cells are highlighted in green color for high RSCU scores (>1.5) and red color for low RSCU scores (<0.5).

AA	Codon	SARS-CoV	SARS-CoV-2	MERS-CoV	HCoV-OC43	HCoV-HKU1	HCoV-229E	HCoV-NL63
A	GCA	1.129	1.09	0.989	1.106	0.917	1.142	1.078
A	GCT	2.069	2.175	2.069	2.159	2.622	2.167	2.395
A	GCC	0.574	0.578	0.631	0.538	0.347	0.467	0.448
A	GCG	0.227	0.157	0.312	0.197	0.114	0.225	0.079
C	TGT	1.265	1.575	1.194	1.534	1.83	1.462	1.821
C	TGC	0.735	0.425	0.806	0.466	0.17	0.538	0.179
D	GAT	1.241	1.275	1.277	1.657	1.704	1.277	1.567
D	GAC	0.759	0.725	0.723	0.343	0.296	0.723	0.433
E	GAA	1.048	1.448	1.052	1.189	1.395	1.407	1.284
E	GAG	0.952	0.552	0.948	0.811	0.605	0.593	0.716
F	TTT	1.231	1.43	1.284	1.752	1.847	1.63	1.802
F	TTC	0.769	0.57	0.716	0.248	0.153	0.37	0.198
G	GGA	0.867	0.791	0.644	0.673	0.418	0.409	0.31
G	GGT	2.015	2.403	2.063	2.492	3.028	2.745	3.33
G	GGC	0.943	0.693	1	0.593	0.405	0.754	0.272
G	GGG	0.175	0.112	0.293	0.242	0.149	0.093	0.088
H	CAT	1.29	1.396	1.32	1.581	1.764	1.457	1.612
H	CAC	0.71	0.604	0.68	0.419	0.236	0.543	0.388
I	ATA	0.625	0.921	0.711	0.97	0.892	0.748	0.676
I	ATT	1.71	1.525	1.718	1.756	1.94	1.878	2.128
I	ATC	0.665	0.554	0.572	0.274	0.167	0.373	0.196
K	AAA	1.042	1.295	1.004	1.041	1.36	1.133	1.203
K	AAG	0.958	0.705	0.996	0.959	0.64	0.867	0.797
L	TTA	1.042	1.63	1.216	1.506	2.397	1.127	1.701
L	TTG	1.084	1.099	1.433	1.928	1.637	2.064	1.838
L	CTA	0.645	0.647	0.459	0.414	0.281	0.355	0.254
L	CTT	1.782	1.763	1.698	1.433	1.324	1.764	1.876
L	CTC	0.84	0.577	0.702	0.297	0.161	0.303	0.208
L	CTG	0.606	0.285	0.492	0.423	0.199	0.387	0.123
N	AAT	1.236	1.36	1.395	1.659	1.742	1.379	1.611
N	AAC	0.764	0.64	0.605	0.341	0.258	0.621	0.389
P	CCA	1.687	1.587	1.219	1.214	0.943	1.326	1.229
P	CCT	1.744	1.973	1.945	2.069	2.605	2.057	2.506
P	CCC	0.406	0.29	0.646	0.503	0.303	0.441	0.174
P	CCG	0.162	0.149	0.19	0.214	0.149	0.176	0.091
Q	CAA	1.174	1.368	1.141	1.072	1.363	1.32	1.344
Q	CAG	0.826	0.632	0.859	0.928	0.637	0.68	0.656
R	AGA	2.082	2.642	1.347	1.84	2.046	2.224	1.427
R	AGG	0.927	0.831	0.842	0.663	0.56	0.628	0.823
R	CGA	0.428	0.3	0.449	0.455	0.342	0.244	0.272
R	CGT	1.739	1.469	1.813	1.977	2.354	2.14	2.894
R	CGC	0.727	0.579	1.114	0.728	0.462	0.635	0.485
R	CGG	0.097	0.18	0.435	0.338	0.236	0.129	0.1
S	AGT	1.172	1.463	1.336	2.075	1.916	1.621	1.947
S	AGC	0.523	0.335	0.437	0.575	0.188	0.504	0.236
S	TCA	1.694	1.666	1.217	0.858	0.869	1.102	1.136
S	TCT	1.959	1.971	2.11	1.84	2.697	2.146	2.343
S	TCC	0.423	0.458	0.712	0.463	0.234	0.479	0.246
S	TCG	0.229	0.108	0.189	0.189	0.097	0.149	0.091
T	ACA	1.571	1.641	1.185	1.27	1.051	1.472	1.204
T	ACT	1.664	1.797	1.952	1.976	2.616	1.904	2.376
T	ACC	0.583	0.38	0.686	0.54	0.249	0.432	0.325
T	ACG	0.182	0.183	0.177	0.214	0.083	0.192	0.095
V	GTA	0.832	0.888	0.724	0.682	0.79	0.445	0.445
V	GTT	1.718	1.984	1.778	2.216	2.726	2.338	2.906
V	GTC	0.668	0.543	0.762	0.318	0.232	0.494	0.332
V	GTG	0.782	0.586	0.736	0.785	0.252	0.723	0.317
Y	TAT	1.122	1.205	1.27	1.669	1.778	1.378	1.629
Y	TAC	0.878	0.795	0.73	0.331	0.222	0.622	0.371

and HCoV-NL63 (28). Thus, it can be stated that high-score and low-score codons are detected in mild category CoVs (except HCoV-229E). We also observed 7 common codons, GCG, GGG, CCG, CGA, CGG, TCG, and ACG, among the 7 CoVs with low RSCU scores. Of these 7 codons, 2 were from the aliphatic group (A-GCG and G-GGG), 1 from the cyclic group (P-CCG), 2 from the basic group (positively-charged) (R-CGA and R-CGG), and 2 from the sulfur-containing groups (S-TCG and T-ACG) (Table 4). Overall, significant differences were observed in the frequencies of 2 glutamine codons (GAG and GAA) in the CoVs in the severe category. In the case of GAG, this codon was lowly expressed in SARS-CoV-2 (0.55) compared to SARS-CoV and MERS-CoVs (0.95 and 0.94, respectively), whereas for GAA, this codon is highly expressed in SARS-CoV-2 (1.44) compared to lowly expressed in SARS-CoV and MERS-CoVs (1.04 and 1.05, respectively).

To understand the evolutionary structure of the CoVs, we obtained an average RSCU value for each codon within the multiple sequences of the same virus (or strain). Next, we created a virus-based 59-dimensional codon feature vector, i.e., RSCU scores of 59 codons. Then, a phylogenetic tree (dendrogram) was constructed using the unweighted pair group method with arithmetic mean (UPGMA), a hierarchical clustering method, based on average linkage [54] algorithm (Fig. 5). Subsequently, the severe- and mild category CoVs were clustered in different clades. SARS-CoV-2 was distantly clustered from the other two CoVs in severe category, and two of the mild coronaviruses, HCoV-OC43

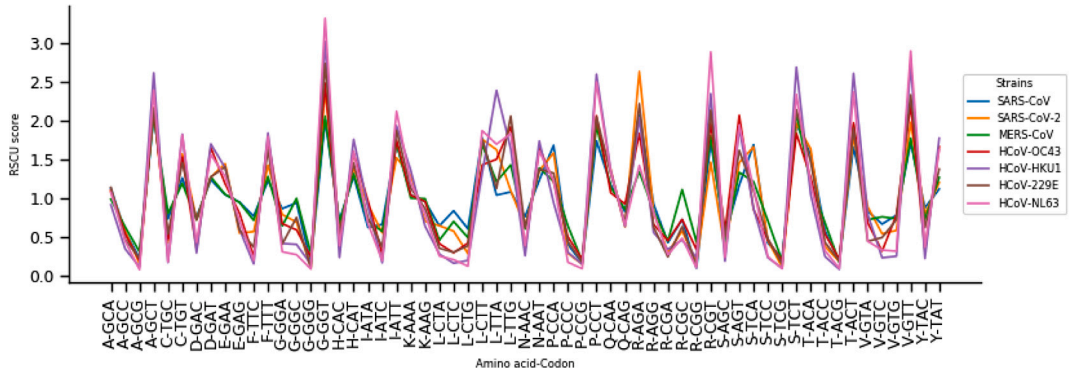

Fig. 4. Distribution of RSCU score for 61 codons mapped to any particular amino acid. The X-axis shows the amino acid one-letter code, followed by synonymous codon (amino acid-synonymous codon), and Y-axis represents the RSCU score.

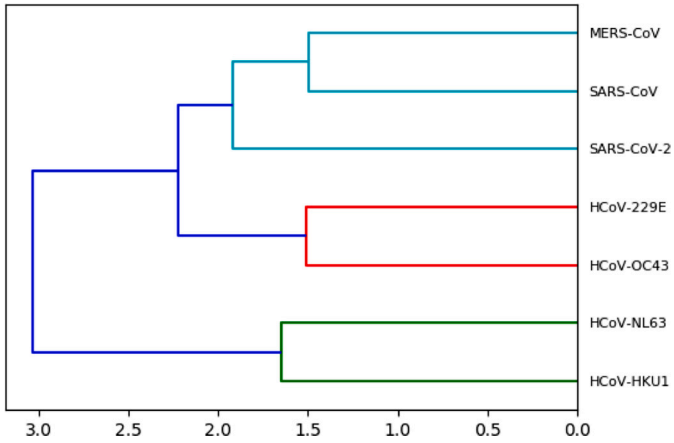

Fig. 5. Phylogenetic correlation of all the seven strains of HCoVs. The tree is constructed using the hierarchical clustering method (UPGMA) and RSCU vectors.

and HCoV-229E, were proximal to severe category CoVs. This finding also indicated a closer codon usage pattern with severe category CoVs (Fig. 4 and Table 4). The principal component analysis of RSCU data also supported the phylogenetic correlations (Fig. 5) of seven CoVs (Supplementary Fig. S1).

Furthermore, we extended our study across 28 different host-virus pairs (Supplementary material 1) that included 18 unique CoVs species targeting 16 different hosts to infer the evolutionary process using codon usage pattern. Next, we constructed the phylogenetic tree of the virus species by applying the same hierarchical clustering method (UPGMA, average linkage) based on the RSCU score. As observed in Figs. 6, 7 candidate HCoVs were distributed into four different clades. The majority of the similar coronaviruses, such as Alpha-CoV 1, Beta-CoV 1, SARS-CoV, and MERS-CoV were collected from different hosts are clustered together. Due to the high sequence similarity among the intragroup species, a similar codon usage pattern was observed, although targeted to different hosts. We also observed one of the evolutionarily close species of SARS-CoV-2, Pangolin-CoV (*Manis javanica*) (same has been confirmed in a previous study [55]). Interestingly, the current analysis highlighted that a possible evolutionary closeness of SARS-CoV-2 with SARS(r)-CoV isolated from the cat host (*Felis catus*).

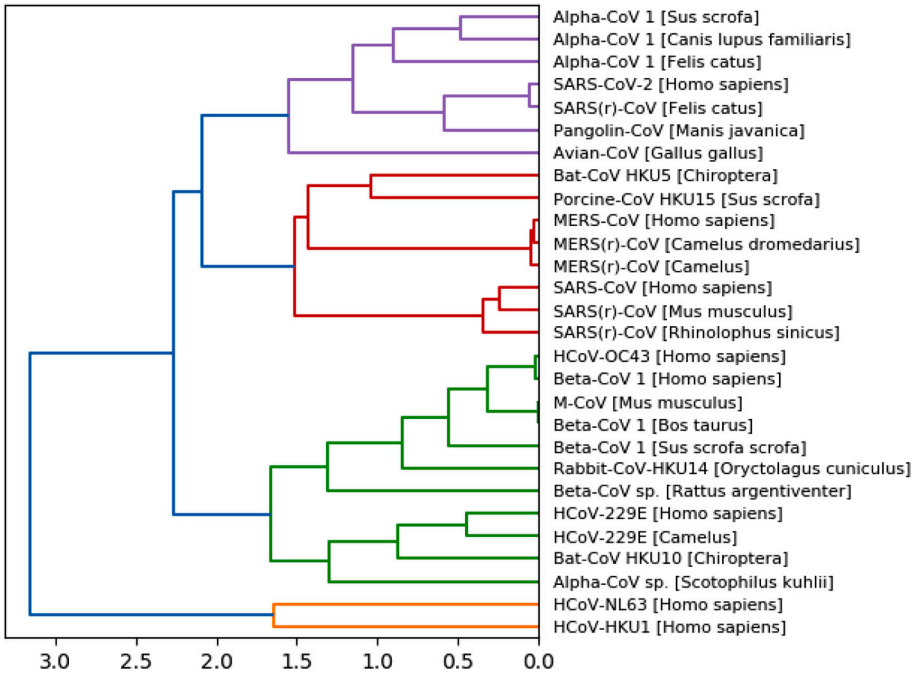

Fig. 6. Hierarchical clustering (UPGMA) of viruses for different hosts representing the phylogenetic correlation obtained utilizing RSCU vectors. A total of 18 distinct CoV species and 16 different hosts representing a total of 28 virus-host pairs.

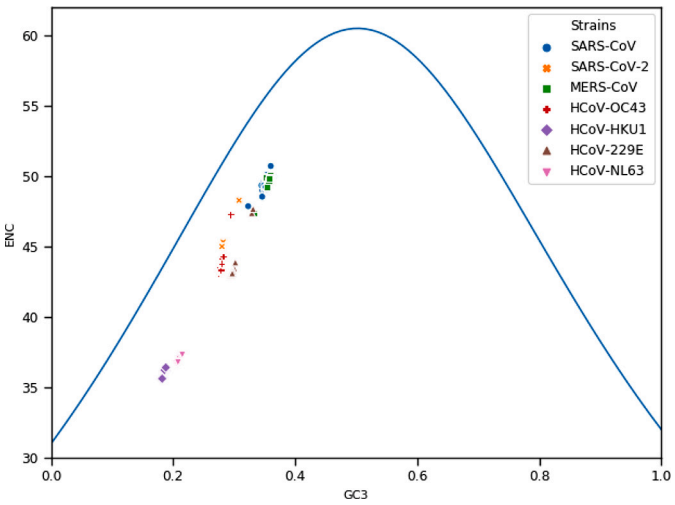

Fig. 7. Ddistribution of ENC values (Y-axis) against GC3 values (X-axis) for all seven CoVs shown in different colors and styles. The ENC curve (blue line) indicaes the expected codon usage. (For interpretation of the references to color in this figure legend, the reader is referred to the web version of this article.)

3.5. Association between ENC and GC3

To assess the potential influence of low or high codon usage bias (*intragenic codon bias*), we calculated the ENC value for all the 7 viruses. Next, we found that the mean ENC value was ranges from 36.40 (for HCoV-HKU1) to 49.8 (for MERS-CoV). An ENC value >45 was considered as a lower codon usage bias. We observed that the mean ENC values for MERS-CoV and SARS-CoV were relatively higher than those of SARS-CoV-2 and other CoVs. Although SARS-CoV-2 showed a high codon usage bias, it could infect other animals, such as cats and ferrets [56]. However, the ENC values for two CoVs (HCoV-OC43 (ENC:43.794) and HCoV-229E (ENC:43.1)) from mild category were higher than the ENC values for the other two mild CoVs (HCoV-229E (ENC:36.4) and HCoV-NL63 (ENC:37.32)). The previous studies on SARS-CoV and MERS-CoV confirmed similar findings [36,51]. Several other studies on different viruses, such as *influenza A* [57], and classical *swine fever* virus [58], reported a low codon usage bias. On the other hand, high codon bias was observed in *hepatitis A* virus [59].

Next, we analyzed the correlation between the ENC value and the GC content in the third site of codons (GC3) in all the 7 CoVs and plotted (Fig. 7). The plot indicated a possible impact of mutational or selection pressure on codon usage [27]. In addition, the ENC curve showed the expected codon usage. We found all the points lying near the solid line on the left region, i.e., observed value was smaller than that of the expected value. These findings suggested that mutational bias might have a role in determining the codon usage variation in candidate viruses. Furthermore, the codon usage bias for severe category CoVs is low. The present study also confirmed the additional role of dinucleotide abundance for the evolution of severe category coronaviruses.

3.6. Neutrality plot and regression analysis

As discussed earlier, a neutrality plot indicates the degree of mutational pressure on codon usage. In synonymous codons, only the last nucleotide differed (except two codons each from arginine, leucine, and serine amino acid). Thus, the nucleotide change at the third position of a codon implies the possible role of mutational force [27,60], rendering that it is an indicator of the extent or the degree of biasness towards base composition [61]. The correlation between GC12 and GC3 could be attributed to mutational forces [62]. Next, we constructed a neutrality plot and a linear regression analysis between GC3 and GC12, between GC3 and GC1, and between GC3 and GC2. First, we showed the distribution of average GC content for the seven strains of HCoVs (Fig. 8 (a)), where we observed various overlapping regions between SARS-CoV-2 and HCoV-229E, SARS-CoV and MERS-CoV, with similar GC content usage pattern. It has also been observed that position-wise distribution might vary among viruses (Fig. 8(b)). The neutrality plot analysis of GC3 against GC1, GC2, and GC12 for all seven CoVs is shown in Fig. 9. The solid line in the figure represents the regression line. The details of the regression line with significant statistical *p*-value and coefficient of determination (R^2) value are shown in Table 5. The slope of the regression line suggests the relative neutrality (mutation pressure) for GC1/GC2/GC12 and the relative constraint on the GC3 (natural selection). Intriguingly, a strong correlation was established between GC12 and GC3 for SARS-CoV-2 ($R^2 = 0.965$, $p < 0.001$) and HCoV-229E ($R^2 = 0.931$, $p < 0.001$) (Table 5), a strong correlation was established between GC12 and GC3 for SARS-CoV-2 [62]. A positive correlation was established between GC3 and GC2 for HCoV-NL63 ($R^2 = 0.81$, $p < 0.001$) and a negative correlation between GC3 and GC1 for HCoV-229E ($R^2 = 0.70$, $p < 0.001$) explicates the role of mutational pressure towards 2nd and 3rd codon position, respectively. Further, we observed a comparatively low correlation between GC3 and GC1 for HCoV-NL63 ($R^2 = 0.48$, $p < 0.001$) and SARS-CoV ($R^2 = 0.37$, $p < 0.001$).

3.7. Comparative host adaptability of different parasites

The host-parasite relation is a complex process and influenced by multiple interacting factors [63]. The viruses are pure parasites and co-evolved with their host. A specific position in the parasite genome may be involved in host-specific adaptations [64] that can exploit the host codon usage [49,65]. The highly expressed viral proteins typically show similar codon usage bias to target host proteins [49,50,66,67]. Similar to viruses, various harmful parasites also cause diseases in humans by the process of host co-adaptation. Therefore, it may be interesting to see how different human parasites including HCoVs, adopt to their hosts by exploiting the host codon usage.

To compare the codon adaptability of different human host parasitic species, we collected a total of 8 species of parasites, 8 species from each of the protozoa (*Plasmodium falciparum, Giardia intestinalis*), bacterium (*Mycobacterium tuberculosis, Bordatella pertussis*), fungus (*Trichophyton rubrum, Trichophyton mentagrophytes*), and virus (*Varicella zoster, Rhinovirus A/B/C)* groups. Next, we compared the codon adaptability score with the above human parasites and the 7 candidate HCoV species. The CAI was calculated using *Homo sapiens* as the reference species and *CAIcal*,[3] a web-server tool. The CAI scores are presented using a box plot for different genes (Fig. 10) and data are reported in supplementary file (Supplementary material 2). We found that CAI scores showed a diverse adaptability pattern among species from the four kingdoms. The CAI in two species of the same group varies except for the fungus group that shows a low CAI score. The CAI scores for the bacteria are relatively higher than other parasites, indicating that bacteria are efficient in adapting to human host. The CAI for viruses showed moderate (0.68–0.72) variations. Among the HCoVs, codon adaptability indicated a diverse adaptability pattern. The CAI value of SARS-CoV-2 is low and closer to SARS-CoV, but both the CAI values were lower than those of MERS-CoV. The low CAI value of SARS- CoV-2 suggested that the gene expression of SARS-CoV-2 was less efficient than that of SARS-CoV, MERS-CoV, and other viruses [36,68,69]. On the other hand, within the mild category, CAI scores show high HCoV-OC43 and HCoV-229E (close to MERS-CoV from severe category) and low HCoV-HKU1 and HCoV-NL63 (close SARS-CoV-2 and SARS-CoV from severe category). This phenomenon indicates that HCoV-OC43 and HCoV-229E have a higher adaptation to the human host and a higher rate of acute respiratory tract infections than other CoVs [70].

[3] https://ppuigbo.me/programs/CAIcal/

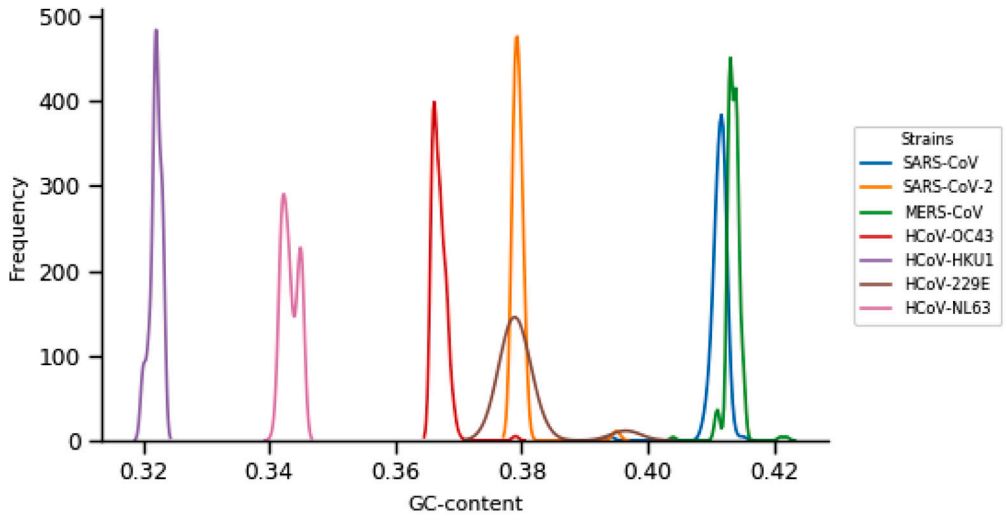

(a)

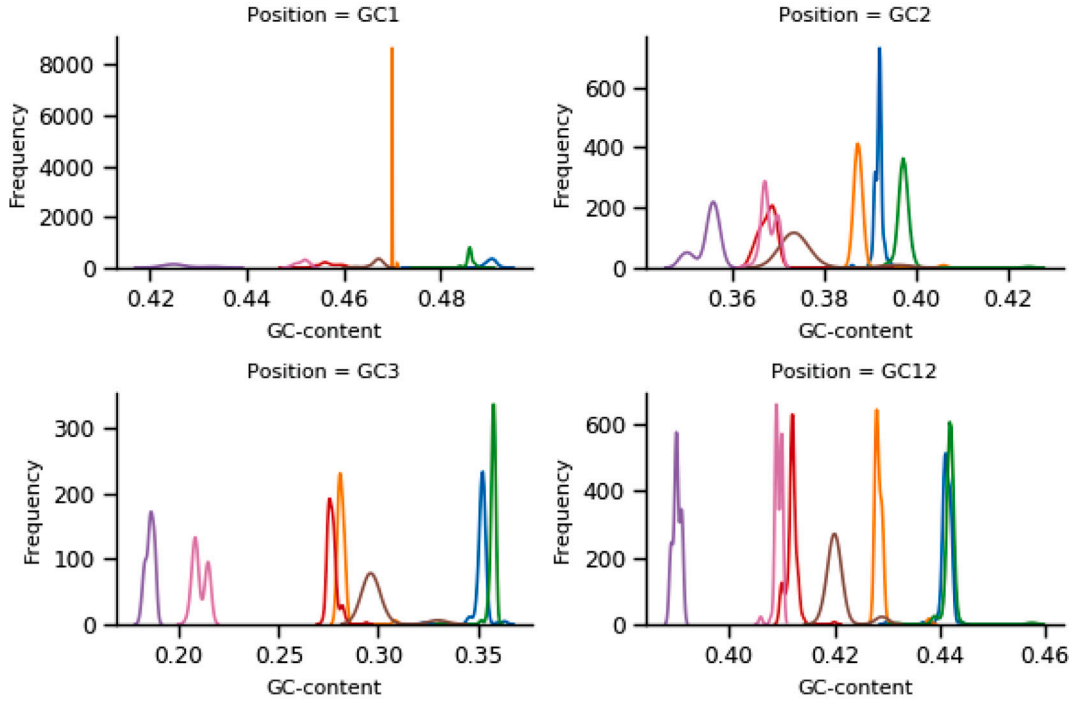

(b)

Fig. 8. (a) The distribution of overall GC-content composition taking all three codon positions for seven human coronaviruses; (b) The position wise distribution of GC-content (GC-content at the first position, Position = GC1; GC-content at the second position, Position = GC2; GC-content at the third position, Position = GC3).

4. Conclusions

We performed an extensive quantitative study on the genome sequence of 7 HCoVs. The critical outcomes of this comparative study on various CoVs have been presented. The percentage of high AT content (58 – 67%) for all CoVs indicates the existence of compositional bias. The current analysis described a high usage of GC and GA dinucleotides (first two positions of codons) and CT dinucleotide (last two positions of codons) that belong to strong hydrogen and pyrimidine groups, respectively. In contrast, CG dinucleotide is low in both cases for all seven CoVs. Next, we observed that the GC content in the third codon position (GC3) in HCoVs. In terms of synonymous codon usage pattern, we observed a high degree of similarity within mild category HCoVs, while in the severe category, the SARS-CoV-2 has the highest codon preference. The common synonymous codon usage for all 7 CoVs was from aliphatic and hydroxyl amino acid groups with high-RSCU values. Simultaneously, low-usage codons are from aliphatic, cyclic, positively-charged, and sulfur-containing groups. A phylogenetic study based on

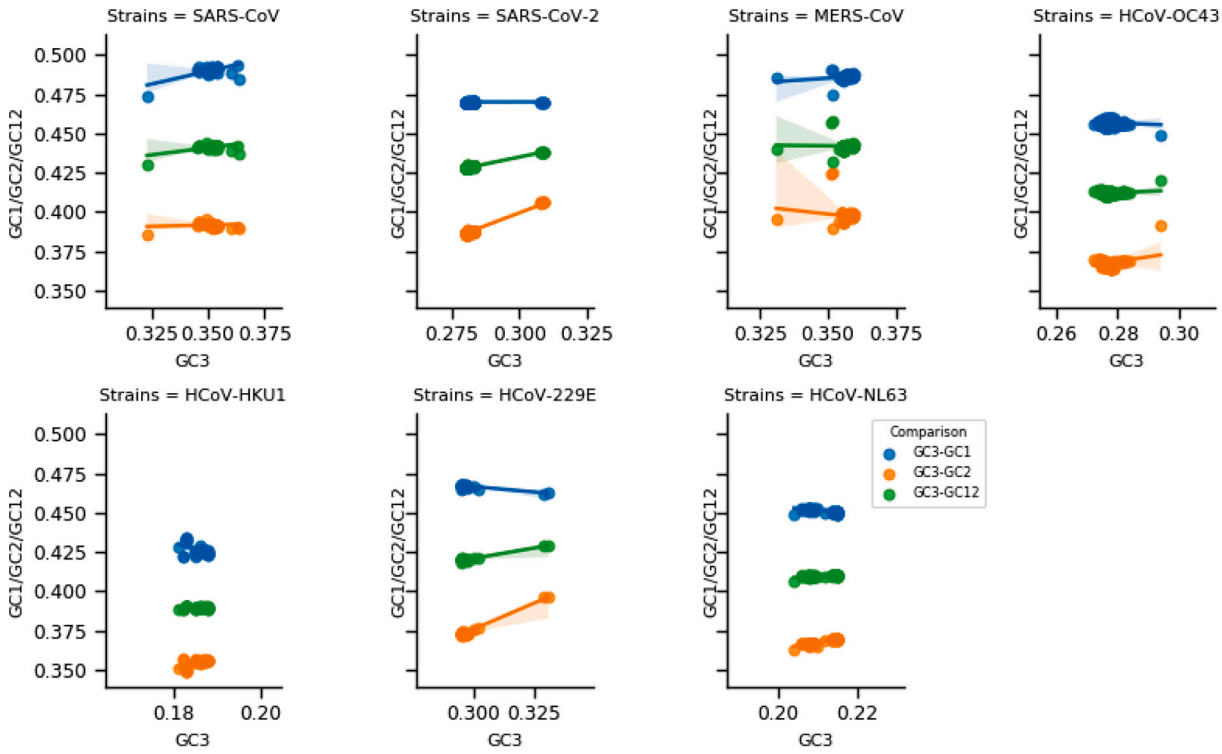

(a)

Fig. 9. The neutrality plot analysis of GC3 against GC1, GC2, and GC12. The solid line represents the regression line.

Table 5
Linear regression computed by comparing GC3 to GC1, GC2 and GC12 for all seven CoVs. The coefficient of determination ($R2$), regression line with a slope, intercept, and p-value are calculated.

Strains	GC3 Vs.	Regression line	R^2	p-value
SARS-CoV	GC1	$y = 0.33x + 0.38$	0.3768	0.0
	GC2	$y = 0.03x + 0.38$	0.0141	0.1713
	GC12	$y = 0.18x + 0.38$	0.2521	0.0
SARS-CoV-2	GC1	$y = 0.00x + 0.47$	0.0005	0.6602
	GC2	$y = 0.65x + 0.20$	0.9659	0.0
	GC12	$y = 0.36x + 0.33$	0.9695	0.0
MERS-CoV	GC1	$y = 0.12x + 0.44$	0.0534	0.0004
	GC2	$y = -0.19x + 0.46$	0.022	0.0236
	GC12	$y = -0.02x + 0.45$	0.0005	0.7275
HCoV-OC43	GC1	$y = -0.08x + 0.48$	0.0098	0.2173
	GC2	$y = 0.30x + 0.28$	0.09	0.0001
	GC12	$y = 0.10x + 0.39$	0.0502	0.0048
HCoV-HKU1	GC1	$y = -0.82x + 0.58$	0.2321	0.0039
	GC2	$y = 0.72x + 0.22$	0.3552	0.0002
	GC12	$y = -0.02x + 0.39$	0.0022	0.7941
HCoV-229E	GC1	$y = -0.14x + 0.51$	0.7023	0.0
	GC2	$y = 0.66x + 0.18$	0.9799	0.0
	GC12	$y = 0.26x + 0.34$	0.9311	0.0
HCoV-NL63	GC1	$y = -0.25x + 0.50$	0.4835	0.0
	GC2	$y = 0.43x + 0.28$	0.8114	0.0
	GC12	$y = 0.11x + 0.39$	0.2866	0.0

RSCU can differentiate between severe- and mild category CoVs. The phylogenetic study with other coronaviruses revealed that the two CoV species isolated from pangolins (*Manis javanica*, pangolin-CoV) and cats (*Felis catus*, SARS(r)-CoV) were in proximity with SARS-CoV-2. It has also been observed that the same CoV species from different hosts are clustered together in the phylogenetic tree that depicts a similar synonymous codon usage pattern. The lowest ENC and CAI values (very close to mild category CoVs) for SARS-CoV-2 clearly indicated a poor adaptation to human codon usage. The overall analysis utilizing different bias indices suggested a potential role of mutation pressure on codon usage, and these findings provide cues for understanding the mechanism of mutations among HCoVs. The analysis of host codon adaptability depicted a lower CAI score for the fungi group and a higher for the bacteria group. Furthermore, CAI scores indicated relatively closer codon adaptability for three coronaviruses, SARS-CoV-2, SARS-CoV, and HCoV-HKU1. Although SARS-CoV-2 exhibits a codon adaptability similar to SARS- CoV, the RSCU-based phylogenetic tree showed proximity among SARS-CoV and MERS-CoV. The current analysis might explain the unique aspects of the virus concerning their resistance to innate immunity and future drug discovery experiments.

Supplementary data to this article can be found online at https://doi.org/10.1016/j.ygeno.2021.05.008.

Author statement

JKD and SR conceived and designed the study. JKD collected the data and performed the computational study. JKD and SR wrote the original manuscript. Both the authors edited and approved for final submission.

Declaration of Competing Interest

Authors declare that they have no conflict of interest.

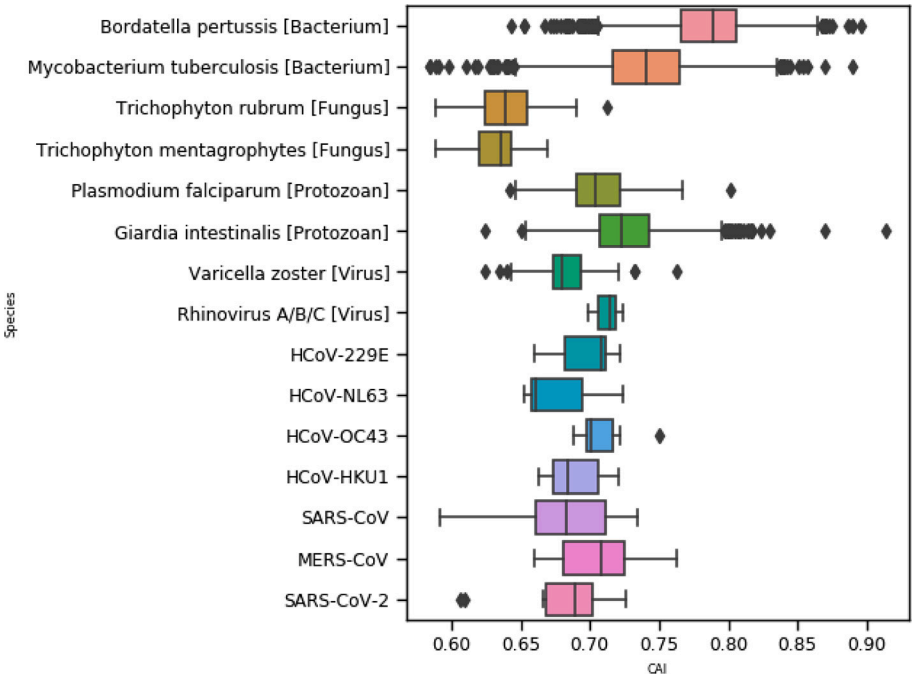

Fig. 10. A box-plot shows the range of codon adaptability indices of 15 different human host parasites (from four kingdoms: virus, fungus, protozoa, bacteria), including seven HCoVs. The CAI range for all protein-coding genes (<20000 bp) of the respective parasite species.

Acknowledgments

The authors thank Dr. Aditi Mitra, Dr. Amit Chakraborty, and Ms. Papia Basu Thakur for their constructive suggestions on improving this manuscript.

References

[1] P.C. Woo, S.K. Lau, C.S. Lam, C.C. Lau, A.K. Tsang, J.H. Lau, R. Bai, J.L. Teng, C. C. Tsang, M. Wang, et al., Discovery of seven novel mammalian and avian coronaviruses in the genus deltacoronavirus supports bat coronaviruses as the gene source of alphacoronavirus and betacoronavirus and avian coronaviruses as the gene source of gammacoronavirus and deltacoronavirus, J. Virol. 86 (2012) 3995–4008.
[2] S. Perlman, J. Netland, Coronaviruses post-sars: update on replication and pathogenesis, Nat. Rev. Microbiol. 7 (2009) 439–450.
[3] J. Peiris, S. Lai, L. Poon, Y. Guan, L. Yam, W. Lim, J. Nicholls, W. Yee, W. Yan, M. Cheung, et al., Coronavirus as a possible cause of severe acute respiratory syndrome, Lancet 361 (2003) 1319–1325.
[4] R.J. de Groot, S.C. Baker, R.S. Baric, C.S. Brown, C. Drosten, L. Enjuanes, R. A. Fouchier, M. Galiano, A.E. Gorbalenya, Z.A. Memish, et al., Commentary: middle east respiratory syndrome coronavirus (mers-cov): announcement of the coronavirus study group, J. Virol. 87 (2013) 7790–7792.
[5] A. Chafekar, B.C. Fielding, Mers-cov: understanding the latest human coronavirus threat, Viruses 10 (2018) 93.
[6] L.E. Gralinski, V.D. Menachery, Return of the coronavirus: 2019-ncov, Viruses 12 (2020) 135.
[7] Y. Ruan, C.L. Wei, A.E. Ling, V.B. Vega, H. Thoreau, S.Y.S. Thoe, J.-M. Chia, P. Ng, K.P. Chiu, L. Lim, et al., Comparative full-length genome sequence analysis of 14 sars coronavirus isolates and common mutations associated with putative origins of infection, Lancet 361 (2003) 1779–1785.
[8] M. Cascella, M. Rajnik, A. Cuomo, S.C. Dulebohn, R. Di Napoli, Features, evaluation and treatment coronavirus (covid-19), in: Statpearls, StatPearls Publishing, 2020 [internet].
[9] E. Tabor, Emerging Viruses in Human Populations, Elsevier, 2006.
[10] J. Lei, Y. Kusov, R. Hilgenfeld, Nsp3 of coronaviruses: structures and functions of a large multi-domain protein, Antivir. Res. 149 (2018) 58–74.
[11] W. Song, M. Gui, X. Wang, Y. Xiang, Cryo-em structure of the sars coronavirus spike glycoprotein in complex with its host cell receptor ace2, PLoS Pathog. 14 (2018), e1007236.
[12] M. Surjit, B. Liu, P. Kumar, V.T. Chow, S.K. Lal, The nucleocapsid protein of the sars coronavirus is capable of self-association through a c-terminal 209 amino acid interaction domain, Biochem. Biophys. Res. Commun. 317 (2004) 1030–1036.
[13] X. Yan, Q. Hao, Y. Mu, K.A. Timani, L. Ye, Y. Zhu, J. Wu, Nucleocapsid protein of sars-cov activates the expression of cyclooxygenase-2 by binding directly to regulatory elements for nuclear factor-kappa b and ccaat/enhancer binding protein, Int. J. Biochem. Cell Biol. 38 (2006) 1417–1428.
[14] Y. Hu, J. Wen, L. Tang, H. Zhang, X. Zhang, Y. Li, J. Wang, Y. Han, G. Li, J. Shi, et al., The m protein of sars-cov: basic structural and immunological properties, Genomics, Proteomics Bioinform. 1 (2003) 118–130.
[15] S. Xia, M. Liu, C. Wang, W. Xu, Q. Lan, S. Feng, F. Qi, L. Bao, L. Du, S. Liu, et al., Inhibition of sars-cov-2 (previously 2019-ncov) infection by a highly potent pan-coronavirus fusion inhibitor targeting its spike protein that harbors a high capacity to mediate membrane fusion, Cell Res. 30 (2020) 343–355.
[16] D.X. Liu, T.S. Fung, K.K.-L. Chong, A. Shukla, R. Hilgenfeld, Accessory proteins of sars-cov and other coronaviruses, Antivir. Res. 109 (2014) 97–109.
[17] C.J. Michel, C. Mayer, O. Poch, J.D. Thompson, Characterization of accessory genes in coronavirus genomes, Virol. J. 17 (2020), https://doi.org/10.1186/s12985-020-01402-1.
[18] S. Osawa, T.H. Jukes, K. Watanabe, A. Muto, Recent evidence for evolution of the genetic code, Microbiol. Mol. Biol. Rev. 56 (1992) 229–264.
[19] S. Herlitze, M. Koenen, A general and rapid mutagenesis method using polymerase chain reaction, Gene 91 (1990) 143–147.
[20] J.K. Das, S. Roy, A study on non-synonymous mutational patterns in structural proteins of sars-cov-2, Genome (2021), https://doi.org/10.1139/gen-2020-0157.
[21] C. Yin, Genotyping coronavirus sars-cov-2: methods and implications, Genomics 112 (5) (2020) 3588–3596.
[22] V.D. Menachery, K. Debbink, R.S. Baric, Coronavirus non-structural protein 16: evasion, attenuation, and possible treatments, Virus Res. 194 (2014) 191–199.
[23] M.C. Zambon, The pathogenesis of influenza in humans, Rev. Med. Virol. 11 (2001) 227–241.
[24] P.J. Walker, J.A. Cowley, Viral genetic variation: implications for disease diagnosis and detection of shrimp pathogens, FAO fisheries, Tech. Paper (2000) 54–59.
[25] R. Grantham, C. Gautier, M. Gouy, R. Mercier, A. Pave, Codon catalog usage and the genome hypothesis, Nucleic Acids Res. 8 (1) (1980) 197.
[26] R.J. Grocock, P.M. Sharp, Synonymous codon usage in *cryptosporidium parvum*: identification of two distinct trends among genes, Int. J. Parasitol. 31 (2001) 402–412.
[27] R. Khandia, S. Singhal, U. Kumar, A. Ansari, R. Tiwari, K. Dhama, J. Das, A. Munjal, R.K. Singh, Analysis of nipah virus codon usage and adaptation to hosts, Front. Microbiol. 10 (2019) 886.
[28] I.S. Belalov, A.N. Lukashev, Causes and implications of codon usage bias in rna viruses, PLoS One 8 (2013), e56642.
[29] J.K. Das, A. Sengupta, P.P. Choudhury, S. Roy, Characterizing genomic variants and mutations in sars-cov-2 proteins from indian isolates, Gene Rep. (2021) 101044, https://doi.org/10.1016/j.genrep.2021.101044.
[30] C. Yin, Dinucleotide repeats in coronavirus sars-cov-2 genome: evolutionary implications, arXiv Preprint (2020) https://arxiv.org/abs/2006.00280 (arXiv: 2006.00280).
[31] P. Auewarakul, Composition bias and genome polarity of rna viruses, Virus Res. 109 (2005) 33–37.
[32] R. Klitting, E.A. Gould, X. De Lamballerie, G+C content differs in conserved and variable amino acid residues of flaviviruses and other evolutionary groups, Infect. Genet. Evol. 45 (2016) 332–340.
[33] J.B. Plotkin, G. Kudla, Synonymous but not the same: the causes and consequences of codon bias, Nat. Rev. Genet. 12 (2011) 32–42.

[34] P.M. Sharp, L.R. Emery, K. Zeng, Forces that influence the evolution of codon bias, Philosophical Trans. Royal Soc B: Bio. Sci. 365 (2010) 1203–1212.
[35] Z. Zhao, H. Li, X. Wu, Y. Zhong, K. Zhang, Y.-P. Zhang, E. Boerwinkle, Y.-X. Fu, Moderate mutation rate in the sars coronavirus genome and its implications, BMC Evol. Biol. 4 (2004) 21.
[36] Y. Chen, Q. Xu, X. Yuan, X. Li, T. Zhu, Y. Ma, J.-L. Chen, Analysis of the codon usage pattern in middle east respiratory syndrome coronavirus, Oncotarget 8 (2017) 110337.
[37] J.D. Ramirez, M. Munoz, C. Hernandez, C. Florez, S. Gomez, A. Rico, L. Pardo, E. C. Barros, A. Paniz-Mondolfi, Genetic diversity among sars-cov2 strains in south america may impact performance of molecular detection, medRxiv 9 (7) (2020) 580.
[38] M.C. Rahalkar, R.A. Bahulikar, Understanding the Origin of 'batcovratg13', a Virus Closest to Sars-Cov-2, 2020.
[39] K.G. Andersen, A. Rambaut, W.I. Lipkin, E.C. Holmes, R.F. Garry, The proximal origin of sars-cov-2, Nat. Med. 26 (2020) 450–452.
[40] C.C. Burns, J. Shaw, R. Campagnoli, J. Jorba, A. Vincent, J. Quay, O. Kew, Modulation of poliovirus replicative fitness in hela cells by deoptimization of synonymous codon usage in the capsid region, J. Virol. 80 (2006) 3259–3272.
[41] D. Kunec, N. Osterrieder, Codon pair bias is a direct consequence of dinucleotide bias, Cell Rep. 14 (2016) 55–67.
[42] P.M. Sharp, W.-H. Li, An evolutionary perspective on synonymous codon usage in unicellular organisms, J. Mol. Evol. 24 (1986) 28–38.
[43] P.M. Sharp, T.M. Tuohy, K.R. Mosurski, Codon usage in yeast: cluster analysis clearly differentiates highly and lowly expressed genes, Nucleic Acids Res. 14 (1986) 5125–5143.
[44] F. Wright, The 'effective number of codons' used in a gene, Gene 87 (1990) 23–29.
[45] P.M. Sharp, K.M. Devine, Codon usage and gene expression level in dictyosteiium discoidtum: highly expressed genes do [prefer optimal codons], Nucleic Acids Res. 17 (1989) 5029–5040.
[46] P. Puigbò, I.G. Bravo, S. Garcia-Vallve, Caical: a combined set of tools to assess codon usage adaptation, Biol. Direct 3 (2008) 1–8.
[47] F. Di Giallonardo, T.E. Schlub, M. Shi, E.C. Holmes, Dinucleotide composition in animal rna viruses is shaped more by virus family than by host species, J. Virol. 91 (2017).
[48] N. Sueoka, Directional mutation pressure and neutral molecular evolution, Proc. Natl. Acad. Sci. 85 (1988) 2653–2657.
[49] I. Bahir, M. Fromer, Y. Prat, M. Linial, Viral adaptation to host: a proteome-based analysis of codon usage and amino acid preferences, Mol. Syst. Biol. 5 (2009) 311.
[50] H. Song, H. Gao, J. Liu, P. Tian, Z. Nan, Comprehensive analysis of correlations among codon usage bias, gene expression, and substitution rate in arachis duranensis and arachis ipaënsis orthologs, Sci. Rep. 7 (2017) 1–12.
[51] W. Gu, T. Zhou, J. Ma, X. Sun, Z. Lu, Analysis of synonymous codon usage in sars coronavirus and other viruses in the nidovirales, Virus Res. 101 (2004) 155–161.
[52] J.K. Das, P. Das, K.K. Ray, P.P. Choudhury, S.S. Jana, Mathematical characterization of protein sequences using patterns as chemical group combinations of amino acids, PLoS One 11 (2016), e0167651.
[53] J.K. Das, R. Singh, P.P. Choudhury, B. Roy, Identifying driver potential in passenger genes using chemical properties of mutated and surrounding amino acids, in: Computational Intelligence and Big Data Analytics, Springer, 2019, pp. 107–118.
[54] R.R. Sokal, A statistical method for evaluating systematic relationships, Univ. Kansas, Sci. Bull. 38 (1958) 1409–1438.
[55] T.T.-Y. Lam, N. Jia, Y.-W. Zhang, M.H.-H. Shum, J.-F. Jiang, H.-C. Zhu, Y.-G. Tong, Y.-X. Shi, X.-B. Ni, Y.-S. Liao, et al., Identifying sars-cov-2-related coronaviruses in malayan pangolins, Nature (2020) 1–4.
[56] J. Shi, Z. Wen, G. Zhong, H. Yang, C. Wang, B. Huang, R. Liu, X. He, L. Shuai, Z. Sun, et al., Susceptibility of ferrets, cats, dogs, and other domesticated animals to sars–coronavirus 2, Science 368 (2020) 1016–1020.
[57] P. Auewarakul, S. Chatsurachai, A. Kongchanagul, P. Kanrai, S. Upala, P. Suriyaphol, P. Puthavathana, Codon volatility of hemagglutinin genes of h5n1 avian influenza viruses from different clades, Virus Genes 38 (2009) 404–407.
[58] P. Tao, L. Dai, M. Luo, F. Tang, P. Tien, Z. Pan, Analysis of synonymous codon usage in classical swine fever virus, Virus Genes 38 (2009) 104–112.
[59] G. Moratorio, A. Iriarte, P. Moreno, H. Musto, J. Cristina, A detailed comparative analysis on the overall codon usage patterns in west nile virus, Infect. Genet. Evol. 14 (2013) 396–400.
[60] H. Chen, S. Sun, J.L. Norenburg, P. Sundberg, Mutation and selection cause codon usage and bias in mitochondrial genomes of ribbon worms (nemertea), PLoS One 9 (2014), e85631.
[61] H. Deka, S. Chakraborty, Insights into the usage of nucleobase triplets and codon context pattern in five influenza a virus subtypes, J. Microbiol. Biotechnol. 26 (2016) 1972–1982.
[62] G.M. Jenkins, E.C. Holmes, The extent of codon usage bias in human rna viruses and its evolutionary origin, Virus Res. 92 (2003) 1–7.
[63] S.E. Evison, Chalkbrood: epidemiological perspectives from the host–parasite relationship, Curr. Opinion Insect Sci. 10 (2015) 65–70.
[64] R. Forsberg, F.B. Christiansen, A codon-based model of host-specific selection in parasites, with an application to the influenza a virus, Mol. Biol. Evol. 20 (2003) 1252–1259.
[65] L. Tian, X. Shen, R.W. Murphy, Y. Shen, The adaptation of codon usage of+ ssrna viruses to their hosts, Infect. Genet. Evol. 63 (2018) 175–179.
[66] M. Dos Reis, L. Wernisch, R. Savva, Unexpected correlations between gene expression and codon usage bias from microarray data for the whole *escherichia coli* k-12 genome, Nucleic Acids Res. 31 (2003) 6976–6985.
[67] J.K. Das, S. Roy, P.H. Guzzi, Analyzing host-viral interactome of sars-cov-2 for identifying vulnerable host proteins during covid-19 pathogenesis, Infection, Genetics and Evolution (2021) 104921, https://doi.org/10.1016/j.meegid.2021.104921.
[68] M. Kandeel, A. Ibrahim, M. Fayez, M. Al-Nazawi, From sars and mers covs to sars-cov-2: moving toward more biased codon usage in viral structural and nonstructural genes, J. Med. Virol. 92 (6) (2020) 660–666.
[69] N. Kumar, D.D. Kulkarni, B. Lee, R. Kaushik, S. Bhatia, R. Sood, A.K. Pateriya, S. Bhat, V.P. Singh, Evolution of codon usage bias in henipaviruses is governed by natural selection and is host-specific, Viruses 10 (2018) 604.
[70] Human respiratory coronavirus hku1 versus other coronavirus infections in italian hospitalised patients, J. Clin. Virol. 38 (2007) 244–250.